7th Canadian Conference on Earthquake Engineering / Montreal / 1995
7ième Conférence canadienne sur le génie paraséismique / Montréal / 1995

Assessment of the Capacity of Existing Beam-Column Connections

A. Biddah[1], A. Ghobarah[2] and T. Aziz[2]

ABSTRACT

Important existing reinforced concrete frames may have been designed and constructed before current seismic design codes were in effect. This paper describes an experimental investigation of the beam-column assemblage of an existing reinforced concrete frame. A reliable seismic evaluation for existing beam-column connections is developed. The test showed that using rigid connection modelling in the analysis of such structures may give misleading results.

INTRODUCTION

There are many multistorey reinforced concrete frame structures that were designed before the availability of current seismic design codes. The lateral resistance of these structures may not be adequate, even for a moderate earthquake, because of the non-ductile reinforcement details. During an earthquake, beam-column connections may experience severe cyclic load reversals. If the joints in a moment resisting frame do not have adequate strength, the overall strength and stiffness of the frame may be adversely affected. The objective of this study is to assess the seismic capacity of existing structures and to develop a realistic modelling for the joints.

CRITERIA USED IN MODELLING OF SPECIMENS

The seismic behaviour of reinforced concrete structures is affected by the ductility of critical regions and by the stiffness and strength distribution. A reliable simulation of seismic behaviour of real structures should take these parameters into account. To retain the ductility similitude, the following parameters are selected to be equal in both the prototype and the specimen:

1- percentages of longitudinal reinforcements,
2- the ratio between the tension and compression reinforcement,
3- mechanical volumetric percentage of confining reinforcement,
4- normalized axial compression force ($N/A_c f_c'$), where N is the axial load on the column, A_c is the

[1] Ph.D. Candidate, Dept. of Civil Engrg., McMaster University, Hamilton, Ont. L8S 4L7
[2] Professor, Dept. of Civil Engrg., McMaster University, Hamilton, Ont. L8S 4L7

gross area of the column and f_c' is the concrete compression strength,
5- shear ratio (M/Vd), where M is moment, V is shear and d is depth of the member,
6- ratio of ultimate shear force resistance values, corresponding to shear and flexural failure modes.

In a previous research at the University of Illinois at Urbana-Champaign (Abrams 1987), it was concluded that one-quarter scale is the minimum scale at which conventional bars and aggregate can be used to have the same force-deformation behaviour.

EXPERIMENTAL PROGRAM

Test description

An existing frame structure, shown in figure 1, is selected for the study. The frame was designed before current seismic codes were available. Because of laboratory space and equipment limitations, a one third scale was chosen. The dimensions of the prototype and the specimen are shown in figure 1. The specimen consists of a beam 1.27 meters long, framing into a column 3.45 meters high at a distance of 1.27 meters from the top. The beam and column ends of the specimen are assumed to correspond to the approximate location of the inflection points of the prototype frame.

Concrete in the existing structure is assumed to have a compressive strength of 21 MPa. The compressive strength of concrete cylinders at the day of testing (42 days) is 22.6 MPa. Grade 400 MPa reinforcing steel is used as the principal steel. Smooth wire size rods are used for the ties. The column transverse reinforcement do not meet the requirement of the CSA CAN3-23.3-M84, 1984 (nor the ACI 318-89). The column and the beam have 30 mm clear cover. The ratio of factored moment of resistance of the column to the nominal moment of resistance of the beam is 1.55 which is higher than the ratio specified by the CSA CAN3-23.3-M84, 1984, which is 1.1. Details of reinforcement are shown in figure 2.

Test setup and instrumentation

The loading setup for the test is shown in figure 3. An axial load, representing the gravity load, is applied to the column and kept constant throughout the test. Reversed cyclic displacements are applied to the free end of the beam (figure 4). The test consists of eleven cycles of loading, three load controlled cycles, followed by eight displacement controlled cycles as shown in figure 5. Two cycles with same applied displacement are repeated then the displacement is increased. The displacement schedule is intended to cause severe drifts to test the inelastic response of the specimen. Twenty four strain gauges are attached to the reinforcing steel in the critical regions of the specimen. Nineteen displacement transducers are used to separate and identify the various types of deformations that make up the total deformation of the beam-column subassemblage. The total deformation of the connection result from; deformation due to shear strain and flexural rotation in the hinging zone, deformation due to shear strain and flexural rotation outside the hinging zone, rotation of the column at the joint, and shear distortion in the joint. All data from load cells, displacement transducers and strain gauges are recorded by a computer controlled data acquisition system (figure 4).

EXPERIMENTAL RESULTS

Crack pattern and failure modes

During the test, the cracking pattern is carefully marked and recorded. Cracking pattern can provide useful information regarding the failure mechanism of the specimen. The main damage occurred in the joint region accompanied by minor damage in the beam. Most of the damage can be attributed to shear action in the joint and flexure-shear action in the beam. At the early stages of the load history, flexural cracks appeared on the face of the joint near the bottom of the beam. These cracks later joined flexural-shear cracks and formed a grid of inclined cracks during the cyclic load reversals. Under subsequent cyclic loading, the longitudinal steel bars in the beam yielded, multiple parallel diagonal cracks occurred at the joint, and the hoops yielded progressively, the joint core concrete was sliced by the parallel cracks in both directions into rhombic blocks, spalling occurred mainly inside the connection. The shear sliding between the blocks was resisted by aggregate interlock and dowel action of the tie and column bars. With subsequent loading, the interlock and dowel actions deteriorated by progressive fracture and crushing of the blocks. The load bearing capacity of the joint core decreased and final failure was reached. The final crack pattern is shown in figure 6.

Although the anchorage length in the specimen satisfies the current code requirement, a bond failure (bond slip) of the beam reinforcement was reached at cycle 9. This is due to the inadequate concrete confinement in the joint region.

Hysteretic behaviour

Hysteretic loops of the applied load versus displacement of the loading point is shown in figure 7. First yielding occurred at 1% storey drift while the maximum load was reached at 2.2% storey drift. The specimen was evaluated in terms of strength as well as ductility. The horizontal lines shown in figure 7 indicate the yielding and the theoretical ultimate load-carrying capacity of the specimen. The theoretical ultimate load was calculated according to the CSA CAN3-A23.3-M84, 1984, where the over-strength effect was considered. Although the theoretical ultimate flexural (P_u = 388 kN) was almost achieved at displacement ductility factor of 2, the degradation of lateral strength became excessive during the cycle of displacement ductility four.

Shear in the joint

To determine the shear force in the joint, the following expression was used:

$$V_t = A_s f_s - V_{col}$$

where

V_t = total shear force in the joint,
A_s = area of beam reinforcement anchored in the column,
f_s = stress in the reinforcement at the beam to column interface,
V_{col} = shear force in the column, obtained by static equilibrium.

The shear force resisted by the transverse reinforcement was calculated using the average strains measured by two strain gauges:

$$V_s = (A_v f_s d)/s$$

where

V_s = shear force resisted by the transverse reinforcement,
A_v = area of transverse tie over a distance s,
f_s = stress in the transverse tie,
d = distance from extreme compression fibre to tension
= reinforcement of the column.

The joint shear force at peak positive beam displacement for different cycles are shown in figure 8. The figure shows that the hoops resisted approximately 2% and 33% of the shear force at the end of the first quarter cycle of displacement ductilities of one and two respectively. The first crack in the joint appeared at shear stress of $0.32\sqrt{f_c'}$, while the maximum contributions of concrete was $0.41\sqrt{f_c'}$ at displacement ductility of one.

Contributions towards storey drift

Contributions of the beam, columns and joint to the total interstorey drift are calculated, (Jirsa et al. 1991), and plotted against the storey drift angle in figure 9. In general, at large deformation levels, an increase in participation of the most damaged element was accompanied by a severe loss of strength. The column contribution, which was largest at the first stages of the test, diminished by the end of the test when joint deformation contributed more to the total drift. After cycle 9, the joint contribution increased rapidly and accounted for 60% of the total drift by the end of the test. The specimen is considered to have failed in cycle 10 due to severe joint distress which was aggravated by hinging in the columns and bond degradation of column bars in the joint. The measurements coincide with the observed joint distress. The significant response of the joint indicates that considering the joint to be rigid in a dynamic analysis may give a misleading results.

CONCLUSIONS

1. The hysteresis loops for the specimen exhibits a rapid degradation in stiffness and strength with progressive cycling of the applied load. After nine cycles of loading, the damage within the joint was so extensive that only 30% of the maximum strength and stiffness remained, and failure of the specimen was assumed. The hysteresis loops show the characteristic pinching effect that is prevalent in reinforced concrete members without special detailing.

2. Extensive damage occurred within the joint region with minor flexural and shear cracking in the beam and flexural cracking in the column. Severe shear cracks within the joint region opened and closed in synchronization with the cyclic load. A large amount of the concrete cover spalled off the joint and concrete crushing took place within the hinge area.

3. The equation given in the current code to calculate the anchorage length does not represent the case of existing joint with inadequate concrete confinement.

4. A dynamic analysis of the existing reinforced concrete frame assuming rigid beam-column joints may underestimate lateral deformation and would be unable to permit joint shear failure.

REFERENCES

ACI Committee 318, 1989, "Building Code Requirements for Reinforced Concrete (ACI 318-89) and Commentary - ACI 318 R-89," American Concrete Institute, Detroit, Michigan.

Daniel P. Abrams, 1987, "Scale Relations for Reinforced Concrete Beam-Column Joints", ACI Structural Journal, Vol. 84, No. 6, pp. 502-512.

CSA-CAN3-A23.3-M84, 1984, "Design of Concrete Structures with Explanatory Notes", Canadian Standards Association, Rexdale, Ontario.

Jirsa, J.O., Alcocer, S.M., 1991, "Reinforced Concrete Frame Connections Rehabilitated by Jacketing", PMFSEL Report No. 91-1, Phil M. Ferguson Structural Engineering Laboratory, the University of Texas at Austin, Texas.

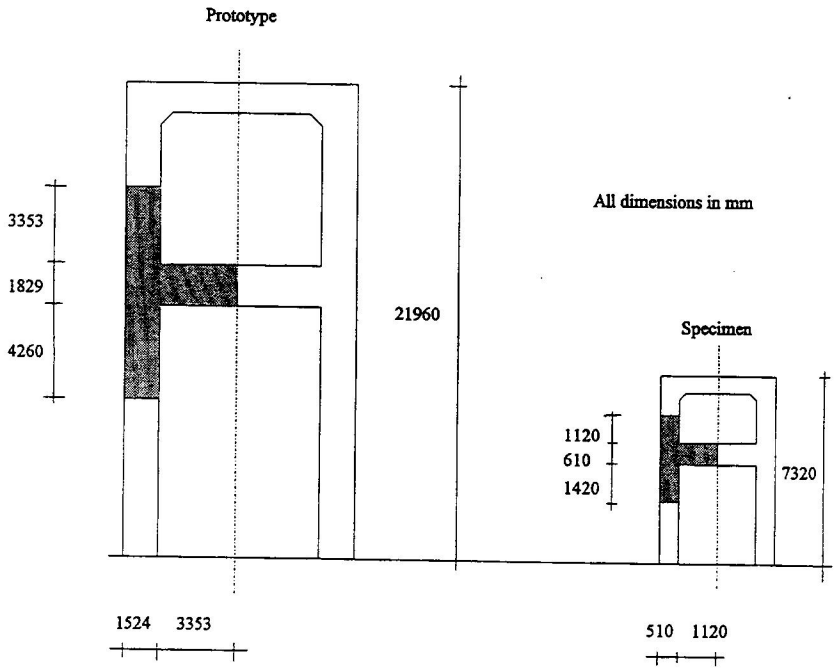

Figure 1 Dimensions of the prototype and the specimen.

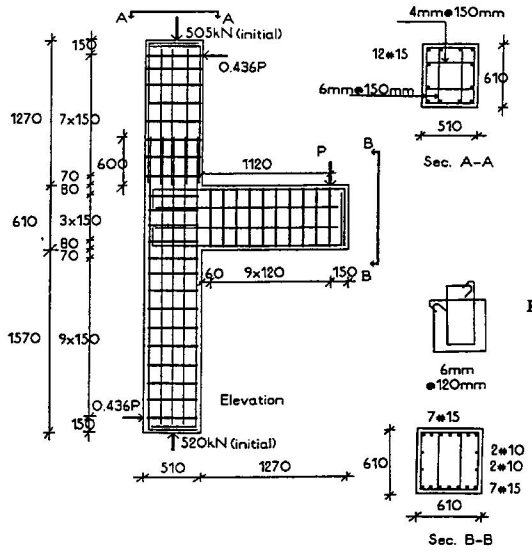

Figure 2 Details of reinforcement of the specimen.

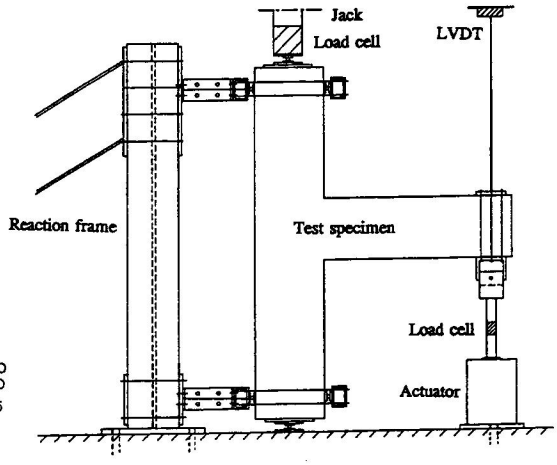

Figure 3 Test setup.

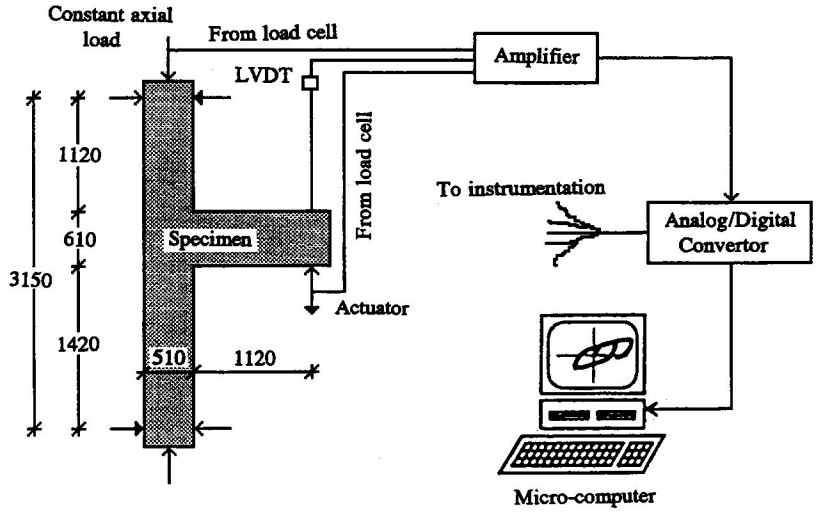

Figure 4 Test specimen and Data acquisition and control systems.

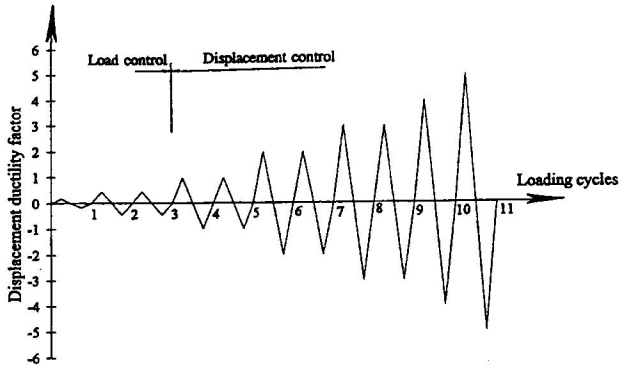

Figure 5 Loading routine.

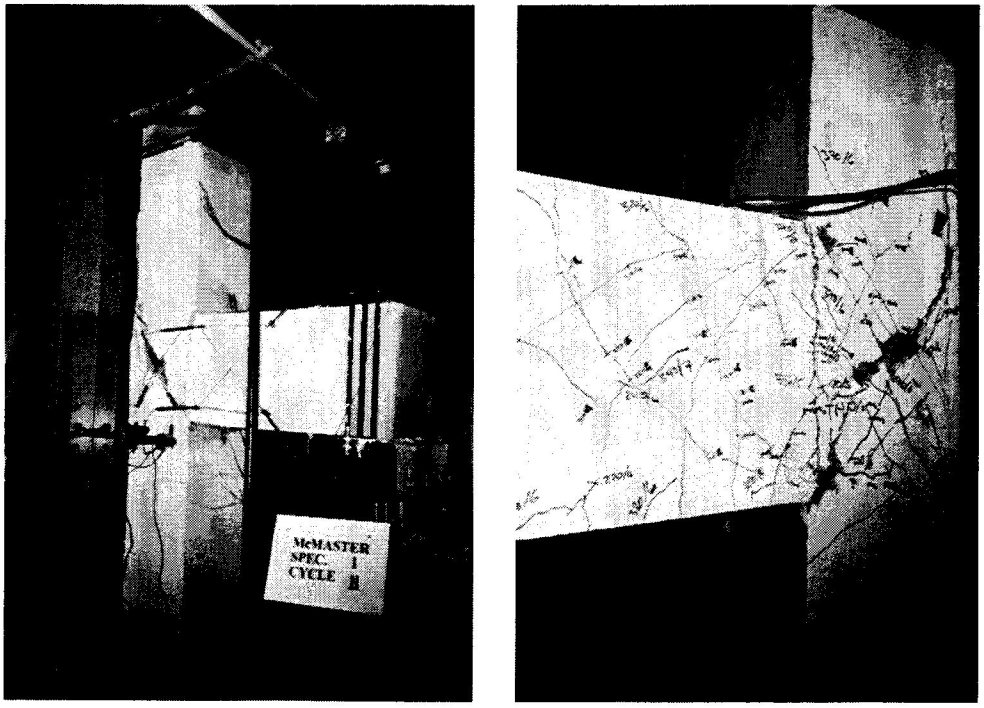

Figure 6 Cracking patterns in specimen.

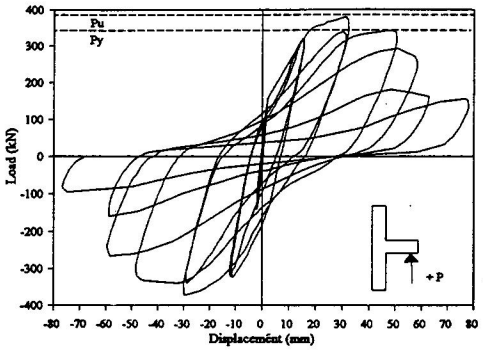

Figure 7 Beam tip load-displacement curves for the specimen.

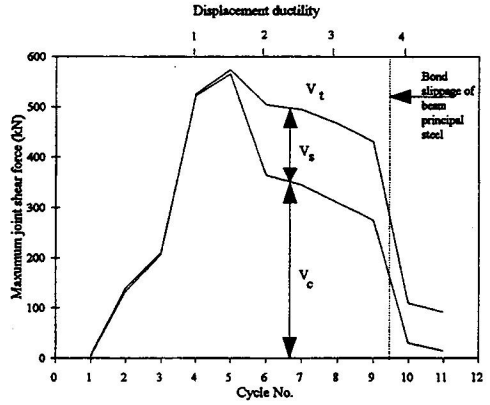

Figure 8 Maximum joint shear force-cycle numbers.

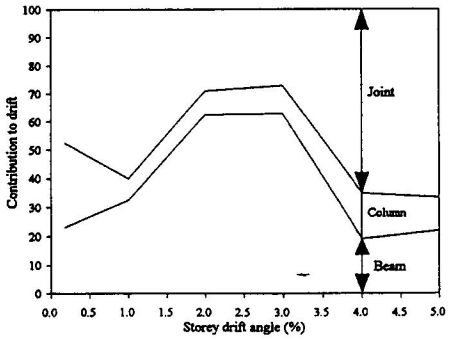

Figure 9 Contribution of members to drift angle.